HHS Public Access

Author manuscript

J Tissue Eng Regen Med. Author manuscript; available in PMC 2020 May 01.

Published in final edited form as:

J Tissue Eng Regen Med. 2019 May ; 13(5): 812–822. doi:10.1002/term.2830.

Scaffolding kidney organoids on silk

Ashwani Kumar Gupta[1], **Jeannine M. Coburn**[2], **Jessica Davis-Knowlton**[1,3], **Erica Kimmerling**[4], **David L. Kaplan**[4], and **Leif Oxburgh**[1,*]

[1]Maine Medical Center Research Institute, Scarborough, ME 04074

[2]Worcester Polytechnic Institute, Worcester, MA 01605

[3]Tufts University School of Medicine, Boston, MA 02111

[4]Tufts University, Medford, MA 02155

Abstract

End stage kidney disease affects hundreds of thousands of patients in the United States. The therapy of choice is kidney replacement, but availability of organs is limited and alternative sources of tissue are needed. Generation of new kidney tissue in the laboratory has been made possible through pluripotent cell reprogramming and directed differentiation. In current procedures, aggregates of cells known as organoids are grown either submerged or at the air-liquid interface. These studies have demonstrated that kidney tissue can be generated from pluripotent stem cells, but they also identify limitations. The first is that perfusion of cell aggregates is limited, restricting the size to which they can be grown. The second is that aggregates lack the structural integrity required for convenient engraftment and suturing or adhesion to regions of kidney injury. In this study we evaluated the capacity of silk to serve as a support for the growth and differentiation of kidney tissue from primary cells and from human induced pluripotent stem cells. We find that cells can differentiate to epithelia characteristic of the developing kidney on this material, and that these structures are maintained following engraftment under the capsule of the adult kidney. Blood vessel investment can be promoted by the addition of VEGF to the scaffold, but the proliferation of stromal cells within the graft presents a challenge, which will require some readjustment of cell growth and differentiation conditions. In summary, we find that silk can be used to support growth of stem cell derived kidney tissue.

Keywords

directed differentiation; fibroin; engraftment

*Author for correspondence: oxburl@mmc.org.

Ethics statement

All animal studies were carried out in compliance with the OLAW “Guide for the care and use of laboratory animals” and approved by the Maine Medical Center IACUC. No human subjects research was performed in this study.

Conflict of interest

The authors declare that they have no conflicts of interest.

Introduction

The Centers for Disease Control reports that approximately 15% of the adult population has chronic kidney disease (http://www.cdc.gov/ckd). This impairment is associated with increased morbidity from multiple causes and frequently progresses to the point at which kidney function is insufficient to sustain physiological homeostasis (Webster et al., 2017). In this state of end stage renal disease (ESRD), patients require kidney replacement therapy. Dialysis with volume regulation provides a means to sustain patients in the short term, but the 5-year survival rate is only 41%. Transplantation is the preferred long-term therapy, and live-donor transplantation is associated with an approximately 87% 5-year survival rate (US Renal Data System 2017 report; https://www.usrds.org). While the purpose of dialysis is to remove urea from the blood, the transplanted kidney regulates levels of many other blood components such as phosphate, calcium, sodium, glucose as well as pH and also functions as a secretory organ (Chen et al., 2017; Curthoys and Moe, 2014; Felsenfeld et al., 2015; Gomez and Sequeira-Lopez, 2018; Hamm et al., 2015; Souma et al., 2015; Subramanya and Ellison, 2014). Given these important differences between dialysis and transplantation, the disparity in survival rates is perhaps not surprising. Ultimately, the nephrology field is working toward regeneration strategies to repair injured kidneys and bioengineering solutions for generating new tissue to increase transplantation access (Oxburgh et al., 2017). These are long-term goals, and a closer prospect may be development of medical devices incorporating both kidney epithelium and urea filtration that could help bridge this important therapeutic gap.

A key question is how to interface kidney epithelium with a solid support. The kidney contains a complex array of epithelial cells organized within the nephron. As blood flows through the glomerulus, water passes through the filtration barrier carrying with it solutes and low molecular weight proteins (Du et al., 2017; Scott and Quaggin, 2015). This solution is conditioned sequentially by proximal tubule epithelial cells, epithelial cells of the loop of Henle, distal tubule epithelial cells, and epithelial cells of the collecting duct. Each one of these distinct epithelial compartments expresses a different combination of transporters, ensuring that water and key molecules are resorbed. Recent advances in directed differentiation of pluripotent human stem cells have demonstrated that generating complex nephron epithelium is feasible (Morizane et al., 2015; Takasato et al., 2015), and have prompted the question: how do we scaffold these developing tissues? Strategies that have previously been used to scaffold kidney cells include decellularized kidney tissue (Caralt et al., 2015; Song et al., 2013) and fibrinogen/collagen I (Homan et al., 2016), and in this study we characterize the properties of silk protein as a scaffolding material for human kidney organoids.

The choice of silk as a support for growth of iPSC-derived kidney cells was motivated by several factors. It is bio-compatible and has been used successfully to support growth of cornea (Gosselin et al., 2018; Lawrence et al., 2009; Siran et al., 2018; Wang et al., 2017), neural tissue (Cairns et al., 2016; Dixon et al., 2018; Tang-Schomer et al., 2014), gastrointestinal tissues (Chen et al., 2015) (Franck et al., 2014; He et al., 2016), and bladder tissue (Chung et al., 2014). Silk has a long history of clinical use as a suture material, and its safety profile in patients is well known. It's in vivo resorption properties can be adjusted so

that it is degraded over the span of a few months to years. Finally, silk can be modified by incorporation of macromolecules. Using this strategy, it is possible to trap essential basement membrane proteins in the scaffold, or to incorporate growth factors which are released over time. In a recent application, we incorporated avidin into the silk scaffolding material so that biotinylated proteins such as growth factors can be conjugated in order to increase their local concentration in the extracellular space (Abbott et al., 2018). Using this type of approach, it is possible both to provide instructive signals to the differentiating tissue within the scaffold and to surrounding tissues at the site of implantation. We are only beginning to understand the requirements for differentiation of kidney tissue from iPSCs, and the versatility of the material provides many possibilities for modification that will allow us to accommodate future developments in differentiation procedures.

We find that induced pluripotent stem cell (iPSC)-derived kidney progenitor cells can be grown to tight densities on this material, and that they undergo epithelial differentiation in response to the WNT/β-catenin activator CHIR99021. Xenografts of synthetic tissue constructs composed of iPSC-derived kidney tissue on silk are vascularized and maintain kidney epithelia *in vivo*. Our data provide a starting point for the development of scaffolding for laboratory-generated kidney tissue, and highlight some pressing challenges for the development of materials for scaffolding kidney tissue.

Materials and Methods

Silk fibroin extraction.

Silk fibroin (hereafter referred to as silk) from *Bombyx mori* silkworm cocoons was extracted as previously described (Rockville et al., 2010). Briefly, cocoons were cut to approximately 1 cm^2 pieces and boiled in 0.02 M $NaCO_3$ for 30 minutes to remove the sericin protein. The resulting silk fibers were rinsed in ultra-pure water (18 mΩ) and air dried overnight. The dry silk fibers were dissolved in 9.3 M LiBr for 3 hours at 60°C then dialyzed against ultrapure water using 3.4 kDa dialysis tubing (ThermoFisher, Waltham, MA) for two days with at least six water changes. The resulting aqueous silk solution was centrifuged at 9,000 rpm for 20 minutes twice and stored at 4°C for future use.

Silk film fabrication.

Silk films were fabricated by air drying 0.3 mL of 5% (w/w) silk solution on 2 cm^2 polydimethylsiloxane (PDMS, Sylgard™ 184, Dow Corning, Midland MI) overnight. The dried silk films were biopsy punched to 4 mm diameter and autoclaved to induce the β-sheet transition and render the silk films water insoluble and sterile.

Silk scaffold fabrication.

Lyophilized silk scaffolds were formed using controlled rate freezing. Briefly, 2 mL of 6% (w/w) silk solution was placed into 15.6 mm diameter cylindrical molds. The silk solution was frozen to −45°C at a rate of −0.25°C/min and then lyophilized at −25°C. The lyophilized silk plugs were autoclaved in glass petri dishes to induce the β-sheet transition and render the silk scaffolds water insoluble.

Cell Culture and directed differentiation

Human iPSCs (WTC11) were maintained in mTeSR™1 (Stem Cell Technologies) in matrigel (Corning) coated six well plate (Corning) in a 37^0C incubator with 5% CO_2. Cells were dissociated with 0.5 M EDTA (Invitrogen) in Ca^{++} and Mg^{++} free PBS (Corning) upon reaching 70–80% confluence and plated in six-well plates with mTeSR™1 containing 10 μM Rho kinase inhibitor, Y27632 (EMD Millipore). After the first 48 hours, Rho kinase inhibitor was removed, and the cells were cultured in unsupplemented mTeSR™1. For directed differentiation, we followed a previously published protocol (Morizane et al., 2015). In Brief, iPSCs were seeded at 1.4×10^4 cells/cm^2 in a 6 well plate. At 50% of confluence, media was replaced with differentiation medium containing Advanced RPMI 1640 (Thermo Fisher Scientific), 1X GlutaMAX™ (Thermo Fisher Scientific), 10 μM CHIR99021 (Reprocell) and 5ng/ml Noggin (R&D Systems). On day 4, cells were cultured with Advanced RPMI 1640, 1X GlutaMAX™ supplemented with 10 ng/ml activin A (R&D). On day 7, cells were cultured with Advanced RPMI 1640, 1X GlutaMAX™ supplemented with 10 ng/ml FGF9 (R&D) for the next two days. On day 9 of directed differentiation, cells derived from human iPSCs represent kidney progenitor cells.

Generation of kidney organoids

Kidney progenitors were harvested with TrypLE Express (Life Technologies) and resuspended at 2.5×10^5 cells/μl in organoid generation medium consisting of STEMdiff™ APEL™ 2 (Stemcell Technologies), 5% PFHM-II (Thermo Fisher Scientific), 100 ng/ml FGF9, 100 ng/ml BMP7 (R&D Systems) and 1 μg/ml Heparin (Sigma). In a 24 well plate, 1 ml/well of organoid generation medium with 8 μM CHIR99021 was added and then Isopore Membrane (EMD Millipore) was suspended at the surface of the medium to create an air-liquid interface by placing on a netwell (Corning Costar). Resuspended cells were aggregated on top of the filter (2 μl/aggregate). On day 2, organoid generation medium containing CHIR99021 was switched to the same medium without CHIR99021 and then cultured for next 12 days. Medium was changed every 3^{rd} day throughout the experiment.

Cell seeding in silk scaffolds

For cell seeding, we used silk scaffolds of 200 μm thickness and 2 mm diameter throughout the study. Hydrated silk scaffolds were sectioned by vibrating microtome at 200 μm, excised using 2 mm biopsy punch (Integra miltex) and autoclaved. One silk disc was transferred in each well of 384 well plate (Greiner bio-one) and then 50 μl media (Advanced RPMI 1640 containing 1X GlutaMAX™ and 10 ng/ml FGF9) with 2.5×10^5 kidney progenitors was added. The plate was centrifuged at 300g for 6 minutes. To check cell seeding efficiency in silk scaffold, we labelled kidney progenitors with DiI (Life Technologies) and, after centrifugation, we used a confocal microscope (Leica, SP8) to image. To observe if the cells were maintained in the scaffold following spin-seeding, we cultured seeded silk in 384 well plate with 50 μl Advanced RPMI 1640, 1X GlutaMAX™ and 10 ng/ml FGF9. On day 3, spin-seeded silks were stained with Phalloidin (Life Technologies #07466) and DAPI using manufacturer's protocol. Stained silks were imaged with confocal microscope.

Differentiation of spin-seeded kidney progenitors

Kidney progenitors were harvested on day 9 of directed differentiation and resuspended at a cell density of 2.5×10^5 per 50 μl in organoid generation media. Cells were spin-seeded in 2mm silk scaffold and transferred to air-liquid interface containing organoid generation media with 8 μM CHIR99021 in 24 well plate. On day 11, organoid generation media was changed without CHIR99021 and then cultured for next 12 days. Media was changed every 3rd day.

Sub-capsular engraftment in mice

To test the effect of VEGF on vascularization, silk scaffolds were soaked in 1μg/ml VEGF (R&D) for 1 hour at room temperature. These VEGF treated silks were engrafted in mice (n=5) under the kidney capsule. On day 7, kidneys were harvested to evaluate vascularization by immunofluorescence staining for endothelial markers. For quantification of $CD31^+$ vessels, Image J software was used to calculate integrated density in five random high-power field (50 μm) Images. Data was analyzed by t-test and GraphPad Prism 5 software was used for statistical analysis. Values expressed as mean ± SE. To study maintenance of differentiated epithelial structures in silk, kidney progenitors were generated through directed differentiation, spin seeded and induced to differentiate. On day 23, differentiated kidney structures in silk scaffolds were first incubated in STEMdiff™ APEL™ 2 supplemented with 1μg/ml of VEGF and then engrafted under kidney capsule of SCID mice. On day 30, engrafted kidneys were harvested for further evaluation.

Immunostaining

Whole mount staining was performed to stain kidney organoids, silk kidney constructs and 100 μm vibratome sections of engrafted kidney. Kidney organoids and silk kidney constructs were fixed in 4% paraformaldehyde in PBS for 15 min at RT in a round bottom 96 well plate whereas engrafted kidneys were fixed in 4% paraformaldehyde for 1 hour per millimeter thickness at 4 ^{0}C before vibratome sectioning. Kidney sections were transferred in flat bottom 96 well plate. After washing with PBS three times, organoids/kidney sections were permeabilized with 1% Triton X100 for 10 min at 4^0 C. 5% donkey serum was used for blocking and then incubated with primary antibodies overnight at 4 ^{0}C. After 6 hours washing with PBS, secondary antibodies with DAPI were incubated for overnight at 4 ^{0}C. After that organoids/silk kidney construct/kidney sections were washed with PBS for 6 hours and mounted with VECTASHIELD antifade mounting medium (Vector Laboratories). For the whole mount staining following antibodies and dilutions were used: rat anti-CDH1 (1:100, Abcam), rabbit Anti-WT1 (1:50, Abcam), goat anti-PODXL (1:100, R&D), BRN1 (1:100, Santa Cruz), rat anti-KRT8 (1:50, The Developmental Studies Hybridoma Bank), rat anti-mouse CD31 (1:50, BD biosciences), rat anti-endomucin (1:100, Abcam), LTL-biotin-conjugated (1:200, Vector Laboratories), DBA-biotin-conjugated (1:200, Vector Laboratories) and rabbit anti-Ki67 (1:100, Abcam). All fluorescent images were taken with a confocal microscope (Leica SP8). For quantification, integrated density of micrographs was measured using Image J. For each antibody stain, 3 separate fields from 3 different organoids or silk scaffolds were measured and the mean was plotted with standard error bars.

Results

Growth of embryonic kidneys and nephron progenitor cells on silk -

To understand if silk is an appropriate support for the growth of embryonic kidney tissue, we cultured embryonic mouse kidneys on sheets of silk suspended at the fluid-air interface of culture medium (Fig. 1A). This “organotypic” culture condition was selected because it vigorously promotes the growth and differentiation of embryonic mouse kidneys (Grobstein, 1953). To understand if the silk material influenced early kidney differentiation *in vitro*, kidneys dissected from E11.5 mouse embryos (Fig. 1A’) were cultured for 48 hours on nuclepore membranes (Fig. 1B) or silk films (Fig. 1C), and immunostained for markers of the branching collecting duct system (KRT8) and nephron progenitor cells (NPCs) (SIX2). Maintenance of the progenitor cell population is an important prerequisite for the differentiation of kidney epithelium on a solid support. We observed vigorous branching of the collecting duct with maintenance of the NPC population at collecting duct tips on both substrates (Figs. 1B’,C’). This observation confirmed that silk is able to support maintenance of undifferentiated SIX2+ NPCs. In the embryonic kidney, SIX2+ NPCs epithelialize in response to WNT/β-catenin signaling, and this is the first step in the formation of the nephron (Carroll et al., 2005). To test the capacity for silk to support this essential mesenchyme to epithelium transition (MET), we seeded purified primary mouse NPCs onto silk scaffolds composed of 6% silk in a sponge configuration with pore sizes between 20 μm and 150 μm. Aiming to mimic the dense packing of NPCs seen in the embryonic kidney within the material, we cultured silk containing NPCs for 10 days in NPC expansion medium (NPEM), which we formulated in previous studies (Brown et al., 2015). SIX2 immunostaining on day 10 after seeding showed that the cells retain expression of this critical transcription factor during this proliferation phase in the silk support (Fig. 1D,D’). Comparison of EdU labeling with the same batch of NPCs cultured in monolayer on Matrigel revealed a similar proliferative index (Fig. 1E,E’), indicating that the silk support is conducive to the proliferation of NPCs in their undifferentiated state. Because we have previously found that MET in the developing kidney does not take place in submerged culture, we transferred the silk supports to nuclepore filters on day 10 after seeding and used the organotypic culture condition shown in Figure 1A for the remainder of the culture period (Fig. 1F). In conjunction with transfer of the scaffold to the filter, we replaced the NPEM with DMEM/F12 containing serum and 5μM of the β-catenin agonist CHIR99021, which mimics the WNT9b/β-catenin epithelialization trigger in the embryonic kidney (Brown et al., 2015). Staining for CDH1 did not reveal any epithelial structures immediately after seeding into silk (Fig. 1G). After 7 days, we found that the silk-supported NPC aggregates converted into epithelia with basolateral E-cadherin (CDH1) staining (Fig. 1H,H’), demonstrating that the silk support is conducive to both the expansion of NPCs in their undifferentiated state and their MET to presumptive nephron epithelia. Based on these observations, we concluded that silk supports the differentiation of kidney tissue from human pluripotent stem cells.

Development of a method to seed PSC-derived kidney tissue into silk supports -

Because human PSCs are fastidious in their growth conditions, we chose not to perform the directed differentiation in the silk, but instead to seed the cells into the silk once the directed

differentiation process was completed in monolayer culture. We developed the seeding method using purified SIX2+ NPCs, and we chose to use the directed differentiation method developed by Morizane et al. (Morizane et al., 2015) because it generates 80–90% SIX2+ NPCs. Because the output of directed differentiation is a mixture of kidney progenitor cells similar to that found in the very early embryonic kidney, it is difficult to define a single growth medium that will enable outgrowth of all cell types. We therefore chose not to employ an undifferentiated expansion phase in the silk material as we did for the primary mouse NPCs. Instead, we developed a method to spin-seed cells from the directed differentiation into silk scaffolds. To fabricate scaffolds, we generated sponges of 6% silk in wells of a 24 well plate, then sectioned these large scaffolds at 200 μm using a vibrating microtome. Then 2 mm discs of scaffolding material were punched out with a biopsy punch; this dimension was selected because it allows culture in a 384 well plate, which is a useful format for screening. In previous work, we characterized these silk scaffolds by scanning electron microscopy and found that the pore size varies between approximately 20μm and 150μm (Oxburgh et al., 2017). Cells were enzymatically detached from culture plates, resuspended at a concentration of 5×10^3 cells/μL and seeded into silk scaffolds at a density of 4×10^5 cells/mm^3 of scaffolding material (Fig. 2A). To demonstrate the efficiency of this approach, we labelled cells with DiI and spin-seeded these cells into scaffolds. Confocal microscopy showed that cells were densely packed into the pockets of the silk scaffold (Fig. 2B). To understand if the cells were maintained in the scaffold following spin-seeding, we cultured them for 3 days and stained with the cytoskeleton marker phalloidin. Cells remained tightly packed in the pockets of the scaffold (Fig. 2C), and we concluded that 300 g centrifugation is efficient to seed the scaffolds.

Kidney progenitor cells derived by directed differentiation of iPSCs give rise to kidney epithelia on silk supports -

Human iPSCs can be differentiated to a mixture of progenitor cells representative of those found in the early embryonic kidney by culturing sequentially in CHIR99021 + noggin, Activin A, and FGF9 over a 9 day period (Fig. 3A) (Morizane et al., 2015). In this protocol, some differentiation of epithelia is seen in submersion culture at the end of the directed differentiation procedure. However, we wanted to encourage vigorous three-dimensional growth of epithelia, and we therefore aggregated the kidney progenitors on day 9 of the directed differentiation protocol on the surface of nuclepore filters (Fig. 1A) and cultured them in organotypic conditions as we previously did with mouse primary NPCs (Fig. 1D–H). We found that epithelial differentiation was inefficient in the advanced RPMI medium used for the directed differentiation procedure and switched to APEL2 with protein-free hybridoma medium (this combination of products is equivalent to the original APEL medium sold by Stemcell technologies). We also found that addition of BMP7, FGF9, and heparin to the culture medium promoted vigorous growth and formation of epithelia.

To test the capacity of silk to support MET of human iPSC-derived kidney progenitors, we compared epithelial differentiation of aggregated kidney progenitor cells with differentiation of kidney progenitor cells spin-seeded into silk scaffolds. MET was initiated by providing a 2 day pulse of the β-catenin agonist CHIR99021, and the medium was subsequently switched to CHIR99021-free for the remainder of the culture period. Cell aggregates clearly

showed clusters of presumptive epithelia by stereo microscopy after 12 days organotypic culture (Fig. 3B), and immunostaining for the tight junction protein CDH1 revealed strong basolateral signal (Fig. 3C, D), supporting the conclusion that cells in the aggregate had undergone MET. hiPSC-derived kidney progenitor cells spin-seeded into silk scaffolds and cultured under identical conditions showed similar formation of epithelia with basolateral CDH1 staining (Fig, 3E–G). Epithelia in both aggregates and silk scaffolds showed evidence of lumen formation (Fig. 3D,G). From this comparison we concluded that the silk material supports MET of hiPSC-derived kidney progenitor cells.

Epithelial structures that differentiate from iPSC-derived kidney progenitors on silk supports express markers of nephron patterning -

To understand which nephron epithelia differentiate from iPSC-derived kidney progenitors on silk, we compared expression of a panel of molecular markers on epithelialized aggregates versus cells epithelialized in silk. Wilms tumor 1 (WT1) and podocalyxin-like (PODXL) label podocytes, and there is similar overlapping expression in aggregates and silk (Fig. 4A,B). Lotus lectin (LTL) and CDH1 label fetal nephron epithelia, with strong LTL labeling in the proximal tubule, and strong CDH1 labeling in the distal tubule; both of these markers were expressed in extensive networks of epithelial tubules on aggregates and silk scaffolds (Fig. 4C,D). POU class 3 homeobox 3 (BRN1) is expressed in epithelial cells of the fetal distal tubule, and was clearly seen in epithelia of both aggregates and silk scaffolds (Fig. 4E,F). Dolichos bifloris agglutinin (DBA) and keratin 8 (KRT8) label collecting duct and connecting tubule in the fetal kidney, and expression was seen in epithelia of both aggregates and scaffolds (Fig. 4G,H). Furthermore, we observed marker transitions in contiguous epithelia in the silk scaffold, indicating that structures were being appropriately patterned (Fig. 4I). Although epithelia arising from human iPSCs appeared less organized than those seen in the fetal kidney, there was clearly appropriate molecular marker expression, supporting the concept that appropriate cell types differentiate in the MET process on silk. This is supported by comparison of integrated density for each marker in aggregates versus silk scaffolds (Fig. 4J). In summary, MET yields a very similar repertoire of differentiated nephron epithelia in silk and in aggregates, and we conclude that the silk material supports differentiation of critical epithelial cell types.

VEGF-treatment increases vascularization of implanted silk scaffolds -

To understand if putative nephron epithelia scaffolded on silk could be maintained *in vivo*, we evaluated their engraftment under the capsule of adult mouse kidneys. Perfusion is essential to the survival of the graft, and because the laboratory-grown scaffolds do not contain any vasculature we first determined whether the silk would recruit vessels in the subcapsular location. Following engraftment of silk scaffolds without cells, we found little evidence of migration of endothelium into the scaffold. To promote the recruitment of endothelium, we treated the silk scaffolds with vascular endothelial growth factor A (VEGF) immediately before engraftment (Fig. 5A,B). We found an approximately 3-fold increase in the recruitment of CD31+ endothelial cells into the scaffolds (Fig. 5C), and we therefore employed this strategy for further engraftment experiments.

Kidney epithelia are maintained in silk scaffolded tissues grafted into adult mouse kidneys

iPSC-derived kidney progenitor cells were prepared as previously described and engrafted under the kidney capsule of SCID mice (Fig. 6A,B). LTL and CDH1 showed maintenance of tubule epithelium with both proximal and distal identities (Fig. 6C); DBA and KRT8 revealed presumptive connecting tubule (Fig. 6D); BRN1 showed distal tubule (Fig. 6E); WT1 and PODXL showed podocytes (Fig. 6F), and endomucin showed endothelium (Fig. 6G), although we found no evidence of glomerular vascularization. While kidney epithelial structures were maintained in the silk, they were less densely packed than prior to engraftment (compare Fig. 4D with Fig. 6C), with a large population of mesenchymal cells interspersed. This suggested that mesenchymal cells were expanding within the graft, marginalizing the putative kidney epithelia. To measure the relative rates of growth, we stained tissues with the proliferation marker Ki67. Indeed, mesenchymal cells were proliferating vigorously, while putative nephron epithelia showed little proliferation, suggesting that the epithelia are being out-competed by mesenchymal cells in the scaffold.

Discussion

Discoveries in directed differentiation and organoid formation support the feasibility of generating kidney tissue de novo in the laboratory from pluripotent stem cells (Morizane et al., 2015; Takasato et al., 2015). Laboratory-generated kidney organoids have found important uses in disease modeling (Cruz et al., 2017; Forbes et al., 2018; Tanigawa et al., 2018). However, to test the capacity of these synthetic tissues to replace lost kidney function in animals, it is important to scale up their size. Scaffolding materials will be important in this endeavor as they can facilitate perfusion, thus removing a key restriction on organoid growth. Furthermore, the structural integrity of silk would facilitate surgical engraftment of synthetic kidney tissue. Our study set out to test whether silk could be a suitable support for iPSC-derived kidney tissue. Based on our studies, we conclude that this material does support growth and differentiation of kidney progenitor cells, but that the expansion of mesenchymal cells represents a technical obstacle.

One important challenge identified in our study is the proliferation of non-epithelial cells in the scaffold. These cells strongly express Meis1 and PDGFRβ and therefore represent a stromal cell population with molecular characteristics of the embryonic kidney interstitium rather than simply undifferentiated pluripotent stem cells. Single cell sequencing of iPSCs differentiated to kidney has revealed an abundance of stromal cells (Wu et al., 2018), and while overabundance of stromal cells is not unique to the silk scaffolding system, limiting their proliferation is critical if we are to increase the density of functional nephron components within the graft to enable effective blood filtration. This work is in progress and our strategies focus on depletion of these cells prior to seeding. Two approaches under development include modification of the organoid culture medium to remove valine, which has been reported to reduce fibroblast proliferation. This is technically relatively challenging as the growth and differentiation characteristics of organoids are complex, and we cannot entirely remove stromal cells because they are required for differentiation of nephrons. Another approach is depletion of the PDGFRβ-expression population using magnetically labeled antibodies. Again, removal of all stromal cells is not feasible, and one of the

challenges is to achieve a reduction rather than a complete removal of the cells. Furthermore, disruption of the cells to a single cell suspension prior to seeding on silk significantly reduces their epithelial differentiation, and we will need to re-adjust growth conditions to compensate for this.

Our study aimed to test if silk is conducive to the growth and differentiation of kidney tissue derived from human pluripotent stem cells, and we have not directly addressed the question of tissue organization. Because of variability in sizes and shapes of the compartments within the silk scaffolds used in this study, both primary NPC-derived and human iPSC-derived tubules appear poorly organized. However, efforts are ongoing to develop silk-based scaffolds with structures that will promote the formation of straight, parallel tubules similar to those seen in the kidney. Technically, generating this type of highly organized structure at the scale of individual human nephrons is challenging.

In this study, we find that silk can be used to scaffold iPSC-derived kidney tissue. In addition to fine-tuning cell culture conditions to reduce the stromal cell burden, our work currently focuses on structural modification, and our primary goal is to reconfigure the scaffold to support the formation of straight tubes of epithelia that more closely model the structure of nephrons.

Acknowledgments

The project described was supported by the National Institutes of Health grant number R24 DK106743 to L.O. and D.L.K., P41 EB002520 (Tissue Engineering Resource Center) to D.L.K., and F32 DK098877 to J.M.C.

References

Abbott A, Oxburgh L, Kaplan DL, Coburn JM, 2018 Avidin Adsorption to Silk Fibroin Films as a Facile Method for Functionalization. Biomacromolecules

Brown AC, Muthukrishnan SD, Oxburgh L, 2015 A synthetic niche for nephron progenitor cells. Developmental cell 34, 229–241. [PubMed: 26190145]

Cairns DM, Chwalek K, Moore YE, Kelley MR, Abbott RD, Moss S, Kaplan DL, 2016 Expandable and Rapidly Differentiating Human Induced Neural Stem Cell Lines for Multiple Tissue Engineering Applications. Stem cell reports 7, 557–570. [PubMed: 27569063]

Caralt M, Uzarski JS, Iacob S, Obergfell KP, Berg N, Bijonowski BM, Kiefer KM, Ward HH, Wandinger-Ness A, Miller WM, Zhang ZJ, Abecassis MM, Wertheim JA, 2015 Optimization and critical evaluation of decellularization strategies to develop renal extracellular matrix scaffolds as biological templates for organ engineering and transplantation. American journal of transplantation : official journal of the American Society of Transplantation and the American Society of Transplant Surgeons 15, 64–75.

Carroll TJ, Park JS, Hayashi S, Majumdar A, McMahon AP, 2005 Wnt9b plays a central role in the regulation of mesenchymal to epithelial transitions underlying organogenesis of the mammalian urogenital system. Developmental cell 9, 283–292. [PubMed: 16054034]

Chen L, Higgins PJ, Zhang W, 2017 Development and Diseases of the Collecting Duct System. Results and problems in cell differentiation 60, 165–203. [PubMed: 28409346]

Chen Y, Lin Y, Davis KM, Wang Q, Rnjak-Kovacina J, Li C, Isberg RR, Kumamoto CA, Mecsas J, Kaplan DL, 2015 Robust bioengineered 3D functional human intestinal epithelium. Scientific reports 5, 13708. [PubMed: 26374193]

Chung YG, Algarrahi K, Franck D, Tu DD, Adam RM, Kaplan DL, Estrada CR Jr., Mauney JR, 2014 The use of bi-layer silk fibroin scaffolds and small intestinal submucosa matrices to support bladder

tissue regeneration in a rat model of spinal cord injury. Biomaterials 35, 7452–7459. [PubMed: 24917031]

Cruz NM, Song X, Czerniecki SM, Gulieva RE, Churchill AJ, Kim YK, Winston K, Tran LM, Diaz MA, Fu H, Finn LS, Pei Y, Himmelfarb J, Freedman BS, 2017 Organoid cystogenesis reveals a critical role of microenvironment in human polycystic kidney disease. Nature materials 16, 1112–1119. [PubMed: 28967916]

Curthoys NP, Moe OW, 2014 Proximal tubule function and response to acidosis. Clin J Am Soc Nephrol 9, 1627–1638. [PubMed: 23908456]

Dixon TA, Cohen E, Cairns DM, Rodriguez M, Mathews J, Jose RR, Kaplan DL, 2018 Bioinspired Three-Dimensional Human Neuromuscular Junction Development in Suspended Hydrogel Arrays. Tissue Eng Part C Methods 24, 346–359. [PubMed: 29739270]

Du B, Jiang X, Das A, Zhou Q, Yu M, Jin R, Zheng J, 2017 Glomerular barrier behaves as an atomically precise bandpass filter in a sub-nanometre regime. Nature nanotechnology 12, 1096–1102.

Felsenfeld AJ, Levine BS, Rodriguez M, 2015 Pathophysiology of Calcium, Phosphorus, and Magnesium Dysregulation in Chronic Kidney Disease. Seminars in dialysis 28, 564–577. [PubMed: 26303319]

Forbes TA, Howden SE, Lawlor K, Phipson B, Maksimovic J, Hale L, Wilson S, Quinlan C, Ho G, Holman K, Bennetts B, Crawford J, Trnka P, Oshlack A, Patel C, Mallett A, Simons C, Little MH, 2018 Patient-iPSC-Derived Kidney Organoids Show Functional Validation of a Ciliopathic Renal Phenotype and Reveal Underlying Pathogenetic Mechanisms. American journal of human genetics 102, 816–831. [PubMed: 29706353]

Franck D, Chung YG, Coburn J, Kaplan DL, Estrada CR Jr., Mauney JR, 2014 In vitro evaluation of bi-layer silk fibroin scaffolds for gastrointestinal tissue engineering. Journal of tissue engineering 5, 2041731414556849.

Gomez RA, Sequeira-Lopez MLS, 2018 Renin cells in homeostasis, regeneration and immune defence mechanisms. Nature reviews. Nephrology 14, 231–245. [PubMed: 29380818]

Gosselin EA, Torregrosa T, Ghezzi CE, Mendelsohn AC, Gomes R, Funderburgh JL, Kaplan DL, 2018 Multi-layered silk film coculture system for human corneal epithelial and stromal stem cells. Journal of tissue engineering and regenerative medicine 12, 285–295. [PubMed: 28600807]

Grobstein C, 1953 Morphogenetic interaction between embryonic mouse tissues separated by a membrane filter. Nature 172, 869–870. [PubMed: 13111219]

Hamm LL, Nakhoul N, Hering-Smith KS, 2015 Acid-Base Homeostasis. Clin J Am Soc Nephrol 10, 2232–2242. [PubMed: 26597304]

He M, Storr-Paulsen T, Wang AL, Ghezzi CE, Wang S, Fullana M, Karamichos D, Utheim TP, Islam R, Griffith M, Islam MM, Hodges RR, Wnek GE, Kaplan DL, Dartt DA, 2016 Artificial Polymeric Scaffolds as Extracellular Matrix Substitutes for Autologous Conjunctival Goblet Cell Expansion. Investigative ophthalmology & visual science 57, 6134–6146. [PubMed: 27832279]

Homan KA, Kolesky DB, Skylar-Scott MA, Herrmann J, Obuobi H, Moisan A, Lewis JA, 2016 Bioprinting of 3D Convoluted Renal Proximal Tubules on Perfusable Chips. Scientific reports 6, 34845. [PubMed: 27725720]

Lawrence BD, Marchant JK, Pindrus MA, Omenetto FG, Kaplan DL, 2009 Silk film biomaterials for cornea tissue engineering. Biomaterials 30, 1299–1308. [PubMed: 19059642]

Morizane R, Lam AQ, Freedman BS, Kishi S, Valerius MT, Bonventre JV, 2015 Nephron organoids derived from human pluripotent stem cells model kidney development and injury. Nature biotechnology 33, 1193–1200.

Oxburgh L, Carroll TJ, Cleaver O, Gossett DR, Hoshizaki DK, Hubbell JA, Humphreys BD, Jain S, Jensen J, Kaplan DL, Kesselman C, Ketchum CJ, Little MH, McMahon AP, Shankland SJ, Spence JR, Valerius MT, Wertheim JA, Wessely O, Zheng Y, Drummond IA, 2017 (Re)Building a Kidney. J Am Soc Nephrol

Scott RP, Quaggin SE, 2015 Review series: The cell biology of renal filtration. The Journal of cell biology 209, 199–210. [PubMed: 25918223]

Siran W, Ghezzi CE, Cairns DM, Pollard RE, Chen Y, Gomes R, McKay TB, Pouli D, Jamali A, Georgakoudi I, Funderburgh JL, Kenyon K, Hamrah P, Kaplan DL, 2018 Human Corneal Tissue

Model for Nociceptive Assessments. Advanced healthcare materials 7, e1800488. [PubMed: 30091220]

Song JJ, Guyette JP, Gilpin SE, Gonzalez G, Vacanti JP, Ott HC, 2013 Regeneration and experimental orthotopic transplantation of a bioengineered kidney. Nature medicine 19, 646–651.

Souma T, Suzuki N, Yamamoto M, 2015 Renal erythropoietin-producing cells in health and disease. Frontiers in physiology 6, 167. [PubMed: 26089800]

Subramanya AR, Ellison DH, 2014 Distal convoluted tubule. Clin J Am Soc Nephrol 9, 2147–2163. [PubMed: 24855283]

Takasato M, Er PX, Chiu HS, Maier B, Baillie GJ, Ferguson C, Parton RG, Wolvetang EJ, Roost MS, Chuva de Sousa Lopes SM, Little MH, 2015 Kidney organoids from human iPS cells contain multiple lineages and model human nephrogenesis. Nature 526, 564–568. [PubMed: 26444236]

Tang-Schomer MD, Hu X, Tupaj M, Tien LW, Whalen M, Omenetto F, Kaplan DL, 2014 Film-based Implants for Supporting Neuron-Electrode Integrated Interfaces for The Brain. Adv Funct Mater 24, 1938–1948. [PubMed: 25386113]

Tanigawa S, Islam M, Sharmin S, Naganuma H, Yoshimura Y, Haque F, Era T, Nakazato H, Nakanishi K, Sakuma T, Yamamoto T, Kurihara H, Taguchi A, Nishinakamura R, 2018 Organoids from Nephrotic Disease-Derived iPSCs Identify Impaired NEPHRIN Localization and Slit Diaphragm Formation in Kidney Podocytes. Stem cell reports 11, 727–740. [PubMed: 30174315]

Wang S, Ghezzi CE, Gomes R, Pollard RE, Funderburgh JL, Kaplan DL, 2017 In vitro 3D corneal tissue model with epithelium, stroma, and innervation. Biomaterials 112, 1–9. [PubMed: 27741498]

Webster AC, Nagler EV, Morton RL, Masson P, 2017 Chronic Kidney Disease. Lancet (London, England) 389, 1238–1252.

Wu H, Uchimura K, Donnelly EL, Kirita Y, Morris SA, Humphreys BD, 2018 Comparative Analysis and Refinement of Human PSC-Derived Kidney Organoid Differentiation with Single-Cell Transcriptomics. Cell stem cell 23, 869–881.e868. [PubMed: 30449713]

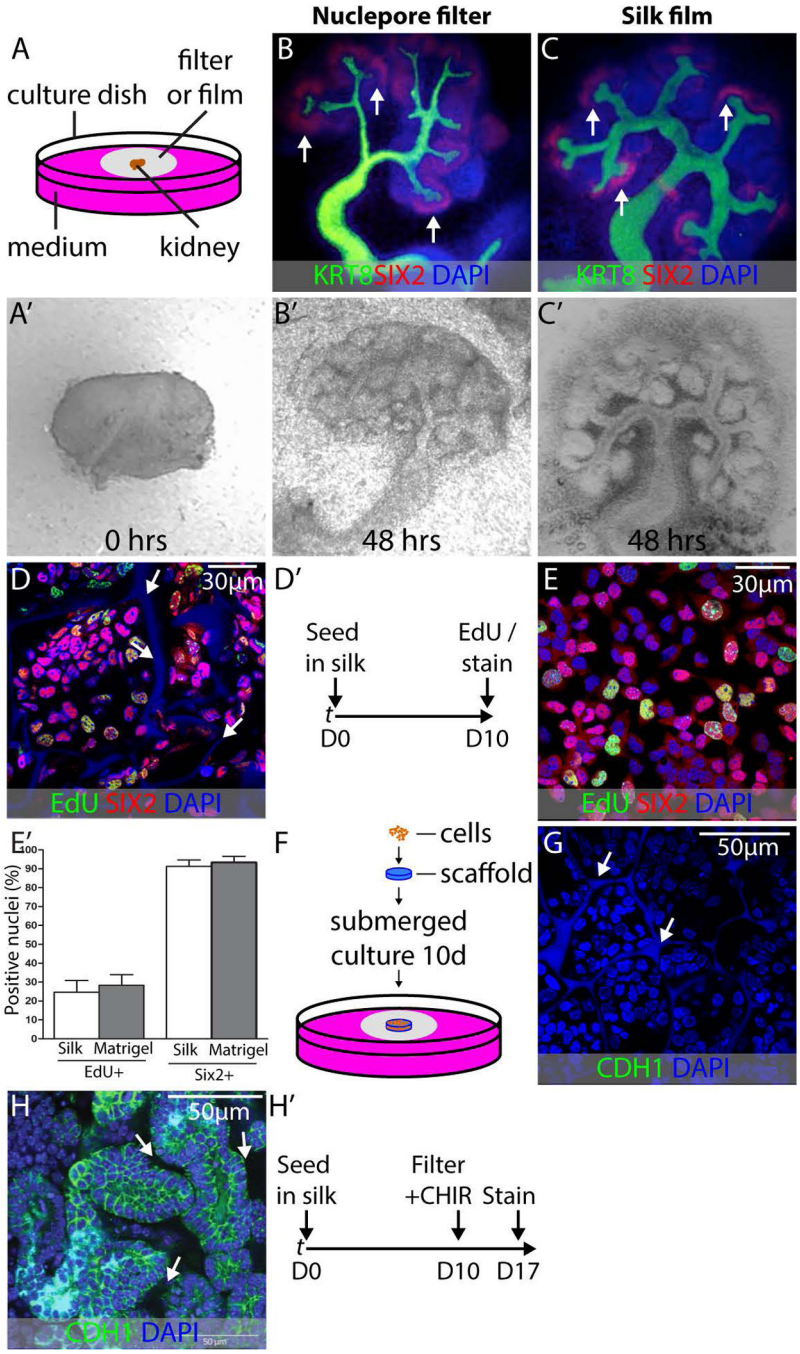

FIGURE 1.

Validation of silk biomaterial for kidney development applications. **(A)** Schematic illustration of embryonic kidney culture in organotypic conditions. All culture experiments were performed in biological triplicate, and representative examples are shown. **(A')** E11.5 kidney imaged on a nuclepore filter at the fluid-air interface immediately after dissection. Note that there is a single epithelial tubule and that there is no branching of the collecting duct. **(B,B')** E11.5 kidney after 48 hours culture in organotypic conditions on nuclepore filter. KRT8 labels collecting duct and SIX2 labels NPCs. Note extensive collecting duct

branching and maintenance of NPCs at collecting duct tips (arrows). **(C,C')** E11.5 kidney after 48 hours culture in organotypic conditions on silk film. Collecting duct branching and NPC maintenance are comparable to culture on nuclepore filter. **(D)** Purified primary NPCs seeded into silk scaffolds and grown in expansion medium for 10 days as shown in (D'). The SIX2 NPC marker is in red, the EdU proliferation marker is in green and the nuclear marked DAPI is in blue. Note the autofluorescence of the silk in the DAPI channel (arrows). (**E**) Purified primary NPCs seeded on Matrigel and grown in expansion medium for 10 days and stained with SIX2, EdU, and DAPI for comparison with silk-seeded NPCs. (**E'**) Quantification of EdU incorporation in NPCs after 10 days growth in silk scaffold versus growth on Matrigel. **(F)** Schematic summarizing the method for loading scaffolds with primary NPCs and subsequently culturing these constructs using organotypic conditions identical to those used for the embryonic kidney. (**G**) Immunostaining for CDH1 to detect epithelial organization in silk scaffolded NPCs on day 1 of the 7 day organotypic culture period. DAPI nuclear counterstain reveals nuclei and silk (arrows) (**H**) Expression of the epithelial marker CDH1 in NPCs expanded in silk scaffolds for 10 days, exposed to CHIR99021 and cultured in organotypic conditions for 7 days. Basolateral CDH1 expression is evident and cells are arranged in typical epithelial structures with lumens. The silk scaffold is within the unstained areas between presumptive tubules (arrows). **(H')** Strategy for outgrowth of NPCs in silk scaffold and subsequent epithelialization.

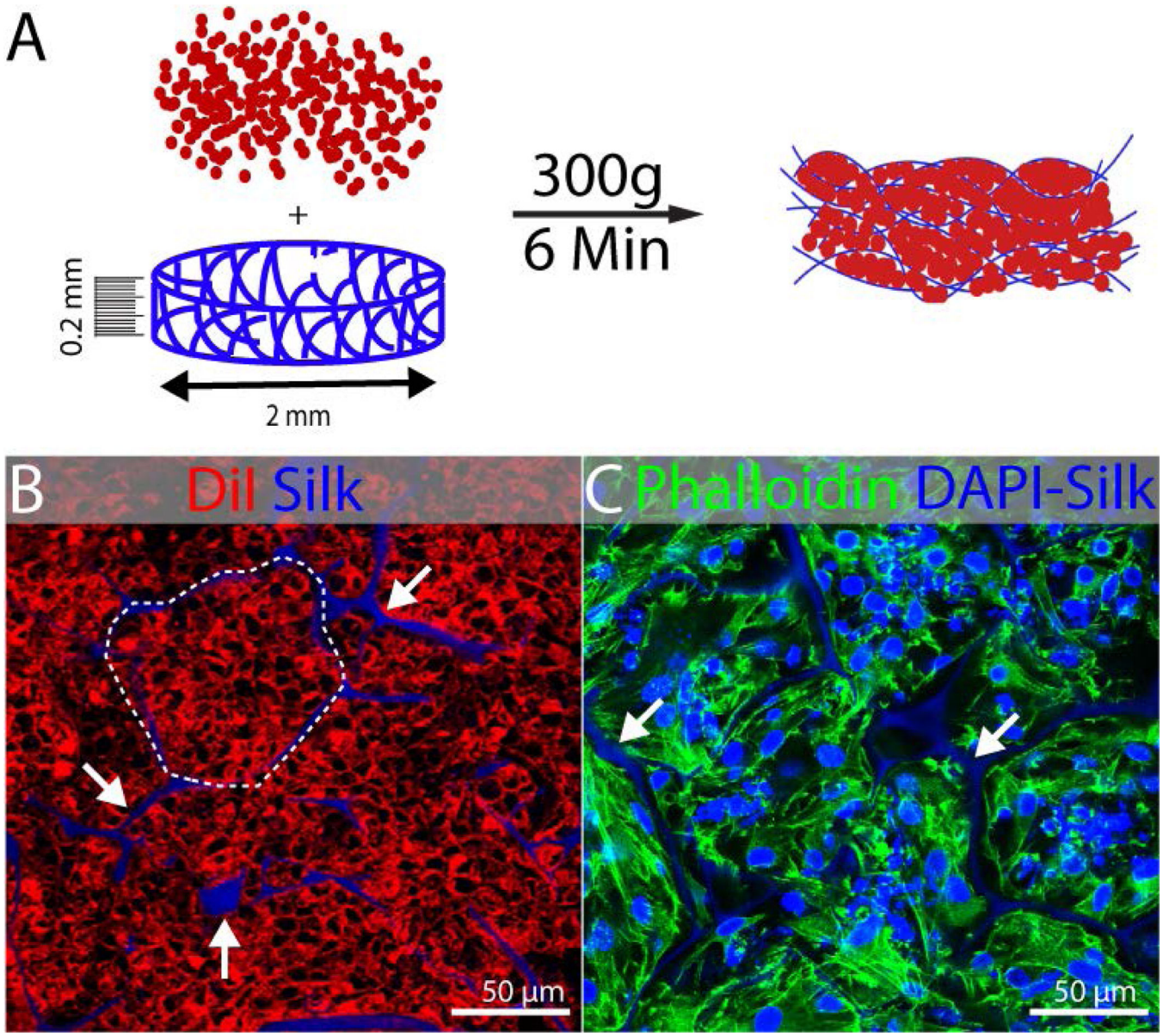

FIGURE 2.

Seeding of kidney progenitors in silk scaffold. Experiments were performed in triplicate and representative examples are shown. **(A)** Schematic illustration of spin-seeding in silk scaffold (0.2mm thick and 2mm diameter) by centrifugation at 300g for 6min. **(B)** Representative fluorescent image showing DiI labeled cells packed (dotted line) into the pockets of silk scaffold (white arrow) after spin-seeding. The DAPI channel was included in this image to show the localization of the autofluorescent silk, although DAPI staining was not performed. **(C)** Phalloidin 488 staining 3 days after seeding showing maintenance of cells packed into the pockets of silk scaffold. DAPI counterstain shows nuclei and the silk scaffold (arrows).

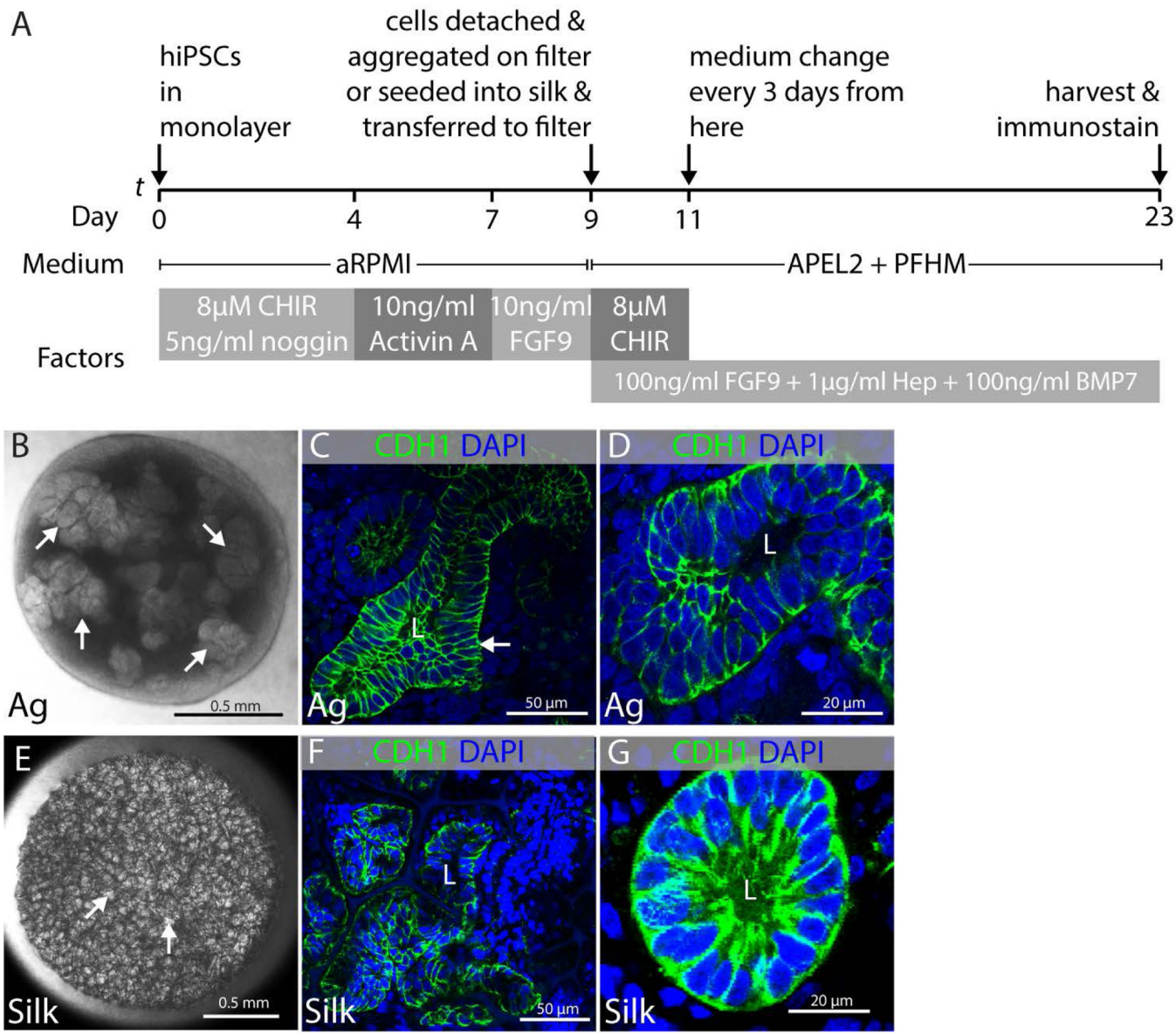

FIGURE 3.

Epithelial differentiation of kidney progenitors. Experiments were performed in triplicate and data representative of a minimum of 3 independent experiments are shown. **(A)** Schematic illustration of protocol showing directed differentiation of hiPSCs into kidney progenitors on day 9 and subsequently into epithelial structures after making aggregates and seeding in silk scaffold. **(B–D)** Epithelial structures that differentiate in aggregates of cells derived from directed differentiation cultured in organotypic conditions. **(B)** Representative stereomicroscope image of kidney organoid generated from hiPSCs at air-liquid interface showing presumptive epithelial clusters (arrows). **(C)** Representative immunofluorescent image showing CDH1+ tubular epithelial structure with lumen (L) in aggregated cells from directed differentiation (arrow). **(D)** High magnification micrograph of epithelial tubule with lumen in aggregated cells from directed differentiation. **(E–G)** Epithelial structures that differentiate in cells from directed differentiation that have been seeded into silk scaffolds.

(E) Representative stereomicroscope image of silk scaffold seeded with cells derived from directed differentiation showing clusters of cells within the pockets of the silk scaffold (arrows). **(F)** Representative immunofluorescent image showing CDH1+ epithelial tubules with lumens (L) within the pockets of the silk scaffold. **(G)** High magnification micrograph of CDH1+ epithelial tubule with lumen (L) within a pocket of the silk scaffold.

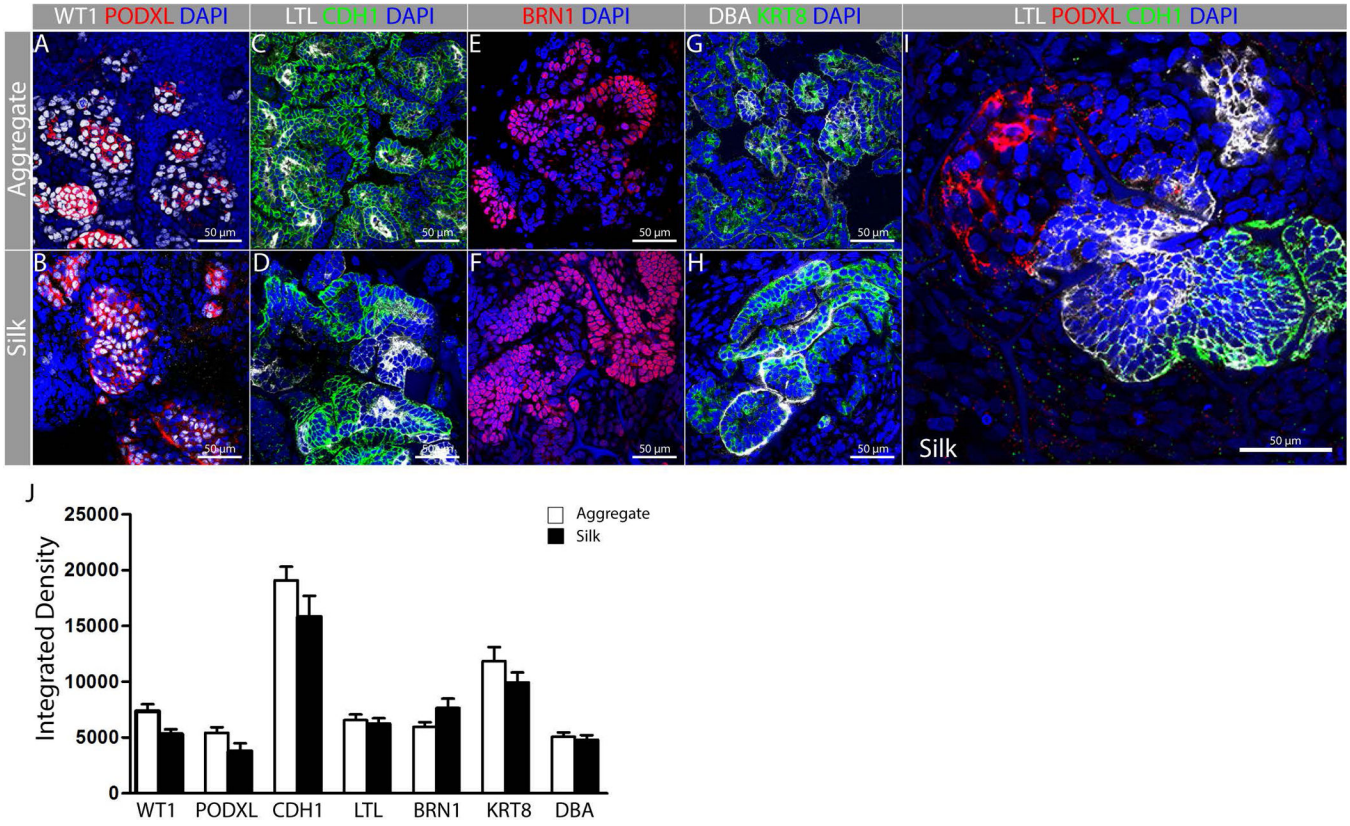

FIGURE 4.

Representative fluorescent images of different nephron segments in aggregates and silk scaffolds. Experiments were performed in triplicate and data representative of a minimum of 3 independent experiments are shown. hiPSC-derived kidney progenitors were cultured either as aggregates **(A, C, E, G)** or cultured in silk scaffolds **(B, D, F, H, I)** as shown in Fig. 3A. Immunostaining was performed for: **(A-B)** Podocytes ($PODXL^+$ $WT1^+$); **(C–D)** Proximal tubule ($CDH1^-$ LTL^+); **(E–F)** Distal tubule ($BRN1^+$) and **(G–H)** Collecting duct ($KRT8^+$, DBA^+). **(I)** Representative fluorescent image showing nephron patterning in presumptive glomerulus ($PODXL^+$), Proximal (LTL^+), distal ($CDH1^+$) and/or collecting duct ($CDH1^+$). **(J)** Quantification of fluorescent intensity for each of the markers used reveals comparable levels of differentiation within the silk scaffold.

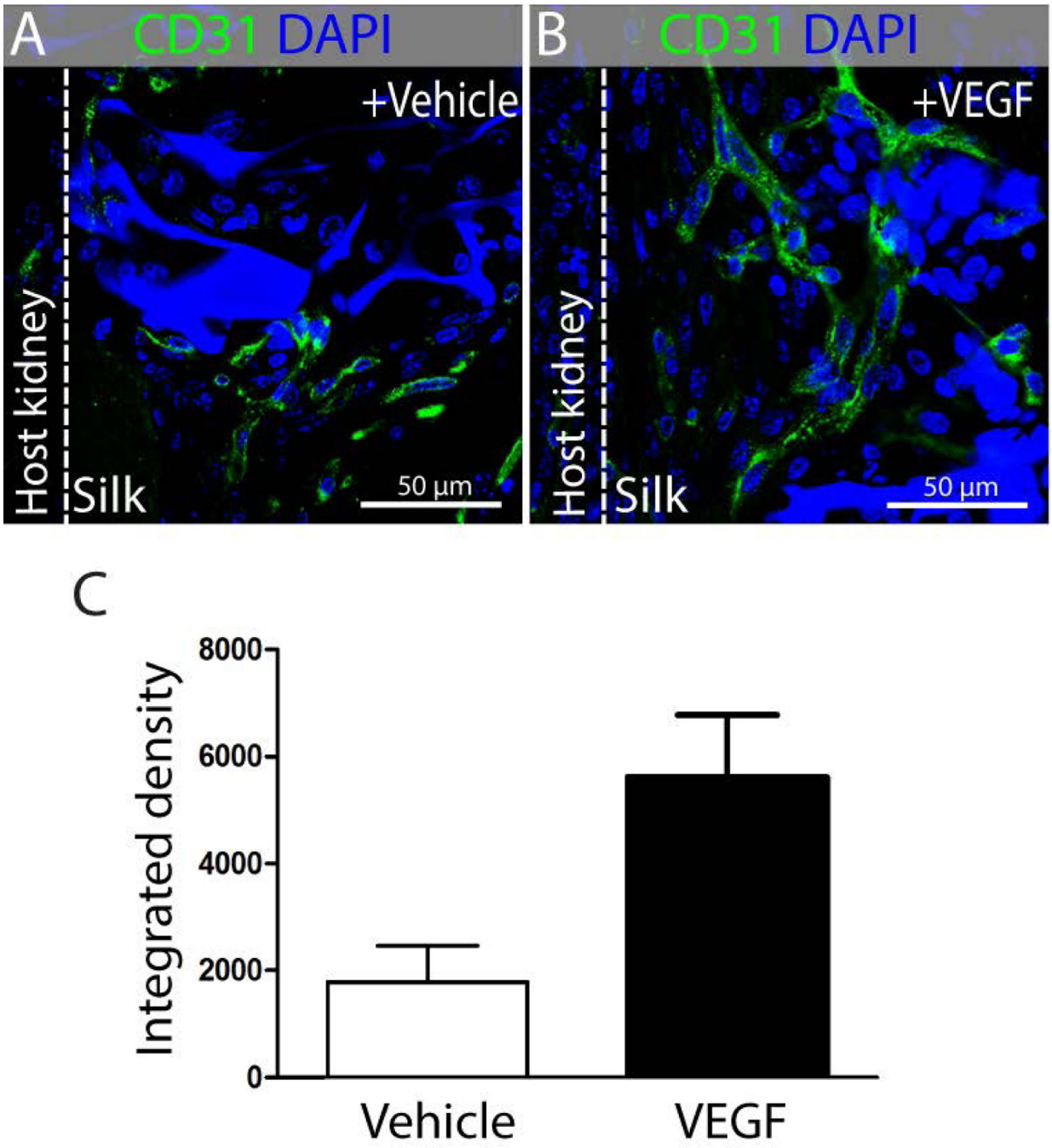

FIGURE 5.

VEGF treatment of silk scaffolds promote vascularization after subcapsular engraftment. Images are representative from n=5 mice in each group. Representative immunofluorescent staining showing $CD31^+$ vasculature in **(A)** vehicle and **(B)** VEGF treated silk scaffold, engrafted under kidney capsule of mice. **(C)** Quantification of $CD31^+$ fluorescence signal in n=5 random high power fields (50µm) from vehicle-treated or VEGF-treated groups.

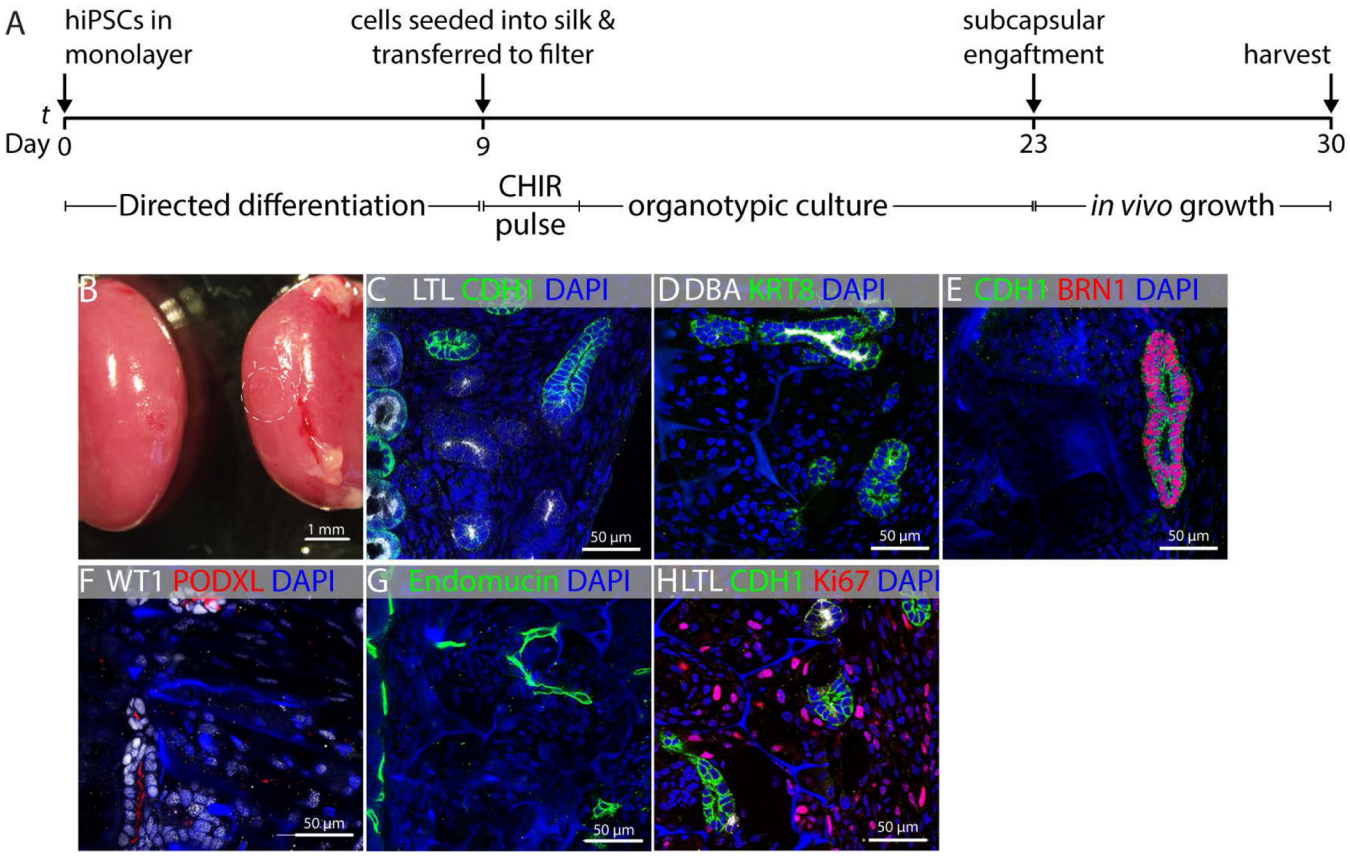

FIGURE 6.

Maintenance of differentiated epithelial structures in vivo. Images are representative from both kidneys of n=3 mice. **(A)** Schematic illustration of work plan showing in vitro differentiation of hiPSC derived kidney progenitors after seeding in silk scaffold and their growth under mice kidney capsule. **(B)** Representative image showing engrafted silk scaffold with differentiated structures under kidney capsule (dotted circle). In vivo engraftment of differentiated renal epithelial structures showing maintenance of **(C)** Proximal tubule ($CDH1^{-}$ LTL^{+}), **(D)** Collecting duct ($KRT8^{+}$, DBA^{+}), **(E)** Distal tubule ($CDH1^{+}$ $BRN1^{+}$) and **(F)** Podocytes ($PODXL^{+}$ $WT1^{+}$). Engrafted silk scaffold with renal epithelial structures were **(G)** vascularized ($Endomucin^{+}$) and **(H)** proliferation ($Ki67^{+}$) of mesenchymal cells was observed in the graft.